Model of Convergent Extension in Animal Morphogenesis

Mark Zajac,* Gerald L. Jones, and James A. Glazier
Department of Physics, University of Notre Dame, Notre Dame, Indiana 46556
(Received 25 January 2000)

We argue that energy minimization can explain the pattern of cell movements in the morphogenetic process known as convergent extension provided that the cell-cell adhesive energy has a certain type of anisotropy, which we describe. This single simple property suffices to cause the cell elongation, cell alignment, and lengthening of a cellular array that characterize convergent extension. We show that the final aspect ratio of the array of cells depends on the anisotropy and is independent of the initial configuration and of the degree of cell elongation.

PACS numbers: 87.18.Ed, 87.18.Hf, 87.18.La

Developing animal embryos greatly change form (morphogenesis) [1]. Some changes involve the coherent motion of groups of cells over distances large compared to cell dimensions. A type of cell rearrangement, termed "convergent extension" is seen in the development of axial structures in a number of, though not all, animal groups. Examples include germ band extension in fruit flies [1], archenteron formation in sea urchins [1], and pronephric duct extension in salamanders [2]. Convergent extension of the axial mesoderm of the frog *Xenopus laevis* has been particularly well characterized by experiments (see [3] for a brief review and extensive references).

In convergent extension an active group of cells undergoes a threefold process. The individual cells, originally roughly isodiametric (Fig. 1a), *elongate* and their axes of elongation become *aligned.* If these were the only motions the final configuration would be as in Fig. 1b. But at the same time, though on a somewhat slower time scale, the cells *intercalate* between each other. The intercalation is in the direction of alignment so that the number of cells in that direction decreases while the number of cells in directions perpendicular to the alignment increases, producing a final configuration as in Fig. 1c. The elongation increases the overall length of the group of cells in the direction of alignment and decreases the length in orthogonal directions (since the volume stays roughly constant). Intercalation does the reverse but dominates, so that the axis of net *extension* of the group of cells is at right angles to the axis of individual cell *elongation*. Here, we argue that these important aspects of convergent extension result from a tendency of the active cells to minimize their total energy, provided that they interact with a nonuniform surface (adhesive) energy satisfying certain conditions. We also develop a mean field theory of this process.

Steinberg [4] suggested that differential cell adhesion and cell motility lead to energy minimization and can account for cell sorting patterns in mixtures of two or more cell types (see [5] for a review and extensive references to the literature). Goel and Leith [6] have considered cell sorting for a simple geometrical model in the presence of anisotropic surface adhesion between cells of fixed shape. Many computer simulations model cell sorting, driven by energy minimization [7,8]. Drasdo, Kree, and McCaskill [9] have simulated cell sorting with anisotropic surface adhesion but not the convergent extension of a homogeneous group of cells. We do not model here the dynamics of convergent extension. We assume, as in [4] and [6], that cell motility will allow the cells to explore possible configurations and that strong dissipation will lead towards the configuration of minimum energy.

In the embryo, convergent extension sometimes takes place in an asymmetric environment where the inactive cells bounding the active region are not the same on all sides. In this case, the boundaries which channel the active cells determine the extension, and its orientation, rather than intrinsic collective properties of the group of active cells. Under these experimental circumstances the boundaries strongly influence active cell movements. Indeed, in the physical model of Weliky *et al.* [10], convergent extension results only if active cells at the boundaries parallel to the elongation behave differently from those at the boundaries perpendicular to the elongation.

A subsequent and elegant experiment by Shih and Keller [11], however, strongly suggests that, in addition, the active cells have an intrinsic collective mechanism driving their convergent extension. In these experiments a layer (essentially a monolayer) of active cells was excised from a frog embryo, at a stage before convergent extension had begun, and grown on a uniform surface in a culture medium. Subsequently the layer showed strong convergent extension in the plane of the substrate, and this in the absence of any plausible lateral anisotropy of the substrate or the culture medium. This behavior appears to be an

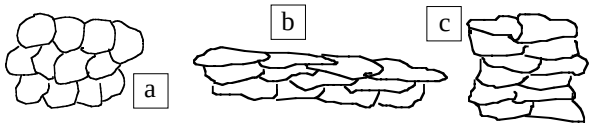

FIG. 1. Intercalation. Isodiametric cells (a) elongate and align (b) while *simultaneously* intercalating (c) so that an array of cells extends at right angles to the direction of cell elongation.

 0031-9007/00/85(9)/2022(4)$15.00

example of "broken symmetry" so well known in condensed matter physics, and asks for an explanation based on collective behavior induced by cell-cell interactions.

To explain this behavior by energy minimization we assume that cell-cell interactions take place through surface adhesion characterized by an energy per unit contact area. We assume that the cell rearrangements take place with negligible cell division, consistent with the later stages of the above experiment. The literature does not identify the trigger for cell elongation and our model does not provide one. Our main assumption is that the adhesive energy of the contact surface between two cells depends on its orientation relative to the axes of elongation of the two cells. For example, the surface density of adhesive binding sites might differ on the long and short sides of a cell or the type of adhesion molecules might differ. We can find in the literature no compelling evidence either for or against this assumption. We argue here that a specific form of this assumption is a sufficient cause of the elongation, alignment, and lengthening characteristic of convergent extension.

Our model is two dimensional since convergent extension takes place in the plane of the substrate. Experiments show that each cell's volume and height remain nearly equal and constant so, in our model, we consider an array of elongated two-dimensional cells, whose areas are all equal and fixed. We assume the array is closely packed (no internal holes) as is observed, and that it contains a large fixed number N of cells. We first want to find the conditions which favor alignment. Figure 2a is a cartoon of a few elongated cells in the interior of such a large ordered array of cells and Fig. 2b is for a disordered array. Suppose that we can roughly distinguish, for each cell, two long sides (parallel to the axis of elongation) and two short sides (perpendicular). Figure 2a shows that in the ordered array the cell-cell contact surfaces are, for the most part, either roughly parallel to the common axes of alignment or roughly perpendicular to the axes. We term these long-long (ll) or short-short (ss) contacts since they occur, primarily, at contacts between a pair of long sides or a pair of short sides. The disordered array of Fig. 2b has many contact surfaces at intermediate angles to the now different axes of adjacent cells. We term these long-short (ls) contacts since they tend to connect a long side of one cell to a short side of a neighbor. If the energy density (per unit length) of the ls contacts is enough larger than those of ll and ss contacts then we expect that the ordered array will have a lower energy per cell. More quantitatively, let l and s be the average long and short side lengths of each cell, which, for the moment, we take as fixed. Suppose that all cell-cell contacts are either ll, ss, or ls and that the total cell-cell contact lengths of each type in the array are L_{ll}, L_{ss}, and L_{ls}. Let S_l be the contact length between long cell sides and the surrounding medium at the array boundary. The N cells have a total long side length $2Nl$. The ll contacts account for $2L_{ll}$ of this since each such contact involves the long sides of two cells. The ls contacts account for L_{ls} and the surface contacts for S_l. Hence $2lN = 2L_{ll} + L_{ls} + S_l$. Similarly, for the short sides, $2sN = 2L_{ss} + L_{ls} + S_s$. We assume that three energy densities (J_{ll}, J_{ss}, and J_{ls}) characterize the cell-cell contacts and that the cell-medium contacts have zero adhesive energy. The array energy is then $E = L_{ll}J_{ll} + L_{ss}J_{ss} + L_{ls}J_{ls}$. Eliminating L_{ll} and L_{ss} between the three equations gives

$$E = L_{ls}\left(J_{ls} - \frac{J_{ll} + J_{ss}}{2}\right) + N(lJ_{ll} + sJ_{ss}) - \frac{S_lJ_{ll} + S_sJ_{ss}}{2}. \quad (1)$$

In a closely packed compact array of N cells, the boundary contact lengths, S, will be proportional to $\sqrt{N}$ while the cell-cell contact lengths L will be proportional to N so the first two terms in Eq. (1) will, to first approximation, dominate for large N. The second term is fixed so that the energy is an increasing function of L_{ls} if the ordering condition,

$$\gamma_{ls} = J_{ls} - (J_{ll} + J_{ss})/2 > 0, \quad (2)$$

is satisfied. In this event ordered arrays ($L_{ls} = 0$) will have lower energies than disordered ($L_{ls} > 0$) arrays, in the limit of large N. Note that condition (2) is that the ls surface tension γ_{ls} be positive.

The above argument is exact if the cells are assumed (unrealistically) to be identical rectangles arranged in arbitrary infinite tesselations of the plane and is similar to that used in [6] for the cell sorting problem. For realistic cells it is a crude but plausible representation.

If a variation in the density of the binding sites on the cell surface causes the variation in adhesive energy and if we make the natural assumption that the density of adhesive bonds is proportional to the product of the density of binding sites on the cell surfaces in contact, then we would have in the above model, $J_{ll} = -j_lj_l$, $J_{ss} = -j_sj_s$, and $J_{ls} = -j_lj_s$, where we choose the sign to make all $J < 0$ when all $j > 0$. This choice satisfies the ordering condition Eq. (2) whenever j_l and j_s are positive and are not equal.

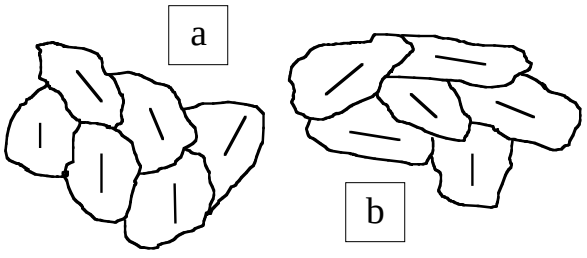

FIG. 2. Cell alignment. For an ordered array (a) most cell attachments are either end to end or side to side while a disordered array (b) exhibits significant binding between poles and lateral surfaces.

In addition to Eq. (2) let us suppose that the ll energy density is lower than the ss energy density:

$$J_{ll} < J_{ss} < 0 \text{ (or } j_l > j_s > 0). \tag{3}$$

Now increasing the cell long side length l and decreasing the short side length s reduces the energy, Eq. (1), causing, or at least favoring, elongation of the cells. At equilibrium these surface effects will presumably balance internal cellular forces opposing further elongation.

We now consider the effect of the boundary on a finite array of N cells. Figure 1 shows, as an example, arrays of twelve elongated cells. In Fig. 1b the array extends in the direction of cell elongation and the boundary contact is primarily at the long sides of cells, so $S_l > S_s$. In Fig. 1c the array extends perpendicular to the cell elongation and the boundary contact is mostly at the short sides, so $S_l < S_s$. If $J_{ll} < J_{ss} < 0$ then Eq. (1) shows that the configuration of Fig. 1c has the lower energy.

For a rectangular array of rectangular cells a direct calculation of the array dimensions D, which minimize the energy, gives $D_\perp/D_\parallel = J_{ll}/J_{ss} > 1$, where $D_\perp$ and $D_\parallel$ are measured along the directions perpendicular and parallel to the cell elongation. We emphasize that this result and also the ordering condition Eq. (2) are independent of the assumption that $l > s$. All of the arguments go through if we interpret the subscripts l and s as simply referring to the cell sides with the lower and the higher adhesive energies. Convergent extension (array extension perpendicular to cell elongation), however, occurs only if $l > s$.

We can make the above arguments concerning surface effects somewhat more realistic and quantitative by the following mean field type of modeling. We assume that we have a large array of N elongated and aligned cells. The total energy of the array is the bulk energy due to cell-cell interactions plus the surface correction for the absence of cells outside the boundary. The bulk energy is proportional to N, or equivalently, the array area A, so we write it as λA, where λ is the (negative) bulk energy per unit area in the aligned array. To model the anisotropic cell-cell interaction we assume that J depends on the angle between the direction of alignment, specified by the unit vector $\hat{\mathbf{a}}$, and the unit vector $\hat{\mathbf{n}}$ normal to the contact segment between the cells (see Fig. 3a). More explicitly, we assume that $J(\hat{\mathbf{n}} \cdot \hat{\mathbf{a}})$ is negative, an even function (since $\hat{\mathbf{a}}$, $-\hat{\mathbf{a}}$ and $\hat{\mathbf{n}}$, $-\hat{\mathbf{n}}$ specify the same physical situations), and is minimum at $\hat{\mathbf{n}} \cdot \hat{\mathbf{a}} = 0$ (so that ll interactions have the lowest energy). Figure 3b shows part of a finite array of vertically aligned cells and their boundary with an external medium with which we assume they have no adhesive energy. To find the energy of the finite array we must subtract from the bulk energy half the energy the boundary cells would have had with cells external to the array had the boundary been absent; half, since adhesive energy is shared between two cells. So

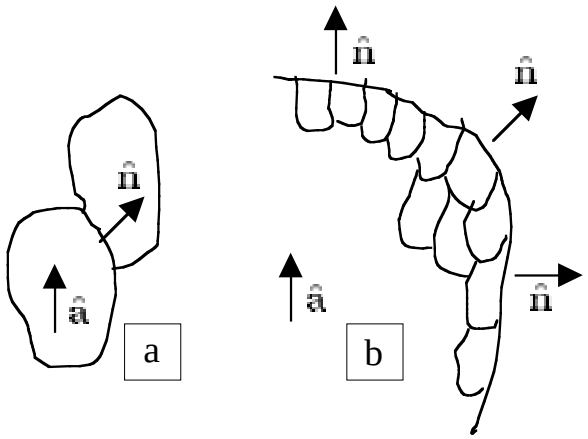

FIG. 3. Anisotropic binding. We assume that the adhesive energy at the point of contact between cells (a) depends on $(\hat{\mathbf{n}} \cdot \hat{\mathbf{a}})^2$ where $\hat{\mathbf{n}}$ is the local unit normal while $\hat{\mathbf{a}}$ gives the alignment, assumed common to all cells. At an interface with uniformly inert surroundings (b), the missing adhesive energy will vary with the orientation of the surface cells relative to the boundary.

$$E = \lambda A - \frac{1}{2}\oint J(\hat{\mathbf{n}} \cdot \hat{\mathbf{a}})\, dl\,, \tag{4}$$

where the integral is taken around a closed boundary. We want to minimize Eq. (4) over all boundaries enclosing the same area A. Alternatively we can interpret λ as a Lagrange multiplier and find the extrema of Eq. (4) over all closed curves at fixed λ. To do this parametrize the curves as $\mathbf{r}(u)$ with $0 \le u \le 1$, and $\mathbf{r}(0) = \mathbf{r}(1)$. Then, since $dl = (\dot{x}^2 + \dot{y}^2)^{1/2} du$ (where $\dot{\mathbf{r}} = d\mathbf{r}/du$), while $(\hat{\mathbf{n}} \cdot \hat{\mathbf{a}}) = (a_y\dot{x} - a_x\dot{y})/(\dot{x}^2 + \dot{y}^2)^{1/2}$ and $A = \int_0^1 y\dot{x}\, du$ we can write the energy as $\int_0^1 \mathcal{L}(\mathbf{r}, \dot{\mathbf{r}})\, du$ with $\mathcal{L}(\mathbf{r}, \dot{\mathbf{r}}) = \lambda y\dot{x} - J(\hat{\mathbf{n}} \cdot \hat{\mathbf{a}})(\dot{x}^2 + \dot{y}^2)^{1/2}/2$. The extremal curves are solutions of the usual Euler-Lagrange equations for $\mathcal{L}$ and are degenerate with respect to translations in the x-y plane. This degeneracy gives rise to two first integrals and two constants of integration (which we choose to be zero), which fix the position of the extremal curve. The integrated equations have the form

$$2\lambda\mathbf{r} = \hat{\mathbf{a}}J'(\hat{\mathbf{n}} \cdot \hat{\mathbf{a}}) + \hat{\mathbf{n}}[J(\hat{\mathbf{n}} \cdot \hat{\mathbf{a}}) - (\hat{\mathbf{n}} \cdot \hat{\mathbf{a}})J'(\hat{\mathbf{n}} \cdot \hat{\mathbf{a}})], \tag{5}$$

where J' is the derivative of J. The dot product of Eq. (5) with $\hat{\mathbf{r}}$ gives the Wulff condition [12]. Equation (5) is two coupled first order differential equations whose solutions depend on the particular choice of the function J. We have not been able to find complete analytic solutions for any interesting choice of J but have found some properties of the solutions. For the simple case of $\hat{\mathbf{a}} = 0$, or equivalently $J = \text{const}$, the solution is a circle of radius $J/(2\lambda)$.

More generally, the turning points of any solution curve occur when $d(\mathbf{r} \cdot \mathbf{r})/du$ vanishes. Now

$$\lambda \frac{d}{du}(\mathbf{r}\cdot\mathbf{r}) = 2\lambda(\dot{\mathbf{r}}\cdot\mathbf{r}) = (\dot{\mathbf{r}}\cdot\hat{\mathbf{a}})J'(\hat{\mathbf{n}}\cdot\hat{\mathbf{a}}), \quad (6)$$

where we have used Eq. (5) and that $\dot{\mathbf{r}}\cdot\hat{\mathbf{n}} = 0$ for any curve. Equation (6) allows two types of turning points: (i) At $\dot{\mathbf{r}}\cdot\hat{\mathbf{a}} = 0$, the boundary is perpendicular to the alignment so that $\hat{\mathbf{n}} = \pm\hat{\mathbf{a}}$. Because J is even and J' is odd, Eq. (5) allows perpendicularity only at the two points $\mathbf{r} = \pm\hat{\mathbf{a}}J(1)/(2\lambda)$, on the line through the origin and parallel to $\hat{\mathbf{a}}$. (ii) At $\hat{\mathbf{n}}\cdot\hat{\mathbf{a}} = 0$ where $J' = 0$, the boundary is parallel to the alignment; Eq. (5) shows that $2\lambda\mathbf{r} = \hat{\mathbf{n}}J(0)$, thus turning points at $\pm J(0)/(2\lambda)$ lie along a line through the origin and perpendicular to $\hat{\mathbf{a}}$. If $D_\perp$ and $D_\parallel$ are the distances between the turning points aligned, respectively, perpendicular and parallel to $\hat{\mathbf{a}}$ then the aspect ratio of the boundary is

$$D_\perp/D_\parallel = J(0)/J(1). \quad (7)$$

If $J(0) < J(1) < 0$ then $D_\perp/D_\parallel > 1$ and the elongation is in the direction perpendicular to the alignment, as observed in convergent extension. From Fig. 3a we see that $J(0)$ corresponds to our previous J_{ll} while $J(1)$ corresponds to J_{ss}.

We have also studied the minimization of the energy functional Eq. (4) numerically for the case where J is chosen to be a Gaussian function. We approximate the boundary curve by a polygon of at least 100 sides and use an iterative process that moves down the energy gradient. We have started from many initial configurations, all of which are closed polygons. The final boundary curve is always the same and has the correct aspect ratio Eq. (7).

Thus, we can understand convergent extension as energy minimization, provided the cell-cell adhesive energy has a certain kind of anisotropy. This single simple property is sufficient cause for the cell elongation, cell alignment, and tissue lengthening that characterize convergent extension. The anisotropy conditions, Eqs. (2) and (3), favor, respectively, the elongation and the alignment of the cells. The final aspect ratio of the cell array is given by Eq. (7) and is independent of both the initial configuration and the degree of cell elongation. Equation (3) also ensures that array extension is perpendicular to cell elongation.

We believe our arguments are plausible but not conclusive. Our modeling neglects many degrees of freedom associated with cell shape and arrangement. Minimizing the bulk and surface energies separately is accurate only for a large array of cells. We do not see much possibility of significant improvement by purely analytic methods. We have initiated simulations of convergent extension, using the Potts model and Metropolis dynamics methods of Refs. [7] and [8], with anisotropic adhesive energies. Anisotropic adhesive energies introduce technical difficulties because the energy becomes nonlocal on the scale of the size of a cell. This considerably increases the simulation time and limits our preliminary results to arrays of 36 cells whereas experimental samples usually contain 100 or more cells. These simulations should still show if the configurations of low energy show the predicted convergent extension. An interesting and more difficult question concerns the simulation dynamics. Will the cells move from an unextended initial state to an extended final state in a sequence of motions similar to that seen in experiment? The answer to this question may well depend on the particular simulation dynamics used to model cell motility. On the experimental side, experiments that probe the possible anisotropy of cell adhesive energy would be useful, as would experiments that show the final configuration is largely independent of the initial configuration.

The authors thank Professor Francois Graner for a helpful discussion.

*Email address: mzajac@krypton.helios.nd.edu

[1] L. Wolpert *et al., Principles of Development* (Oxford University Press, New York, 1998).
[2] J. Drawbridge and M. S. Steinberg, Int. J. Dev. Biol. **40**, 709 (1996).
[3] R. Keller and J. Shih, in *Interplay of Genetic and Physical Processes in the Development of Biological Form at the Frontier of Physics and Biology*, Proceedings of the Les Houches Summer School, edited by D. Beysens, G. Forgacs, and F. Gail (World Scientific, Singapore, 1995), pp. 143–153.
[4] M. S. Steinberg, Science **141**, 401 (1963).
[5] F. Graner, J. Theor. Biol. **164**, 455 (1993).
[6] N. S. Goel and A. G. Leith, J. Theor. Biol. **28**, 469 (1970).
[7] F. Graner and J. A. Glazier, Phys. Rev. Lett. **69**, 2013 (1992).
[8] J. A. Glazier and F. Graner, Phys. Rev. E **47**, 2128 (1993).
[9] D. Drasdo, R. Kree, and J. S. McCaskill, Phys. Rev. E **52**, 6635 (1995).
[10] M. Weliky, S. Minsuk, R. Keller, and G. Oster, Development **113**, 1231 (1991).
[11] J. Shih and R. Keller, Development **116**, 887 (1992).
[12] G. Wulff and Z. Kristall, Mineral **34**, 449 (1901); I. V. Markov, *Crystal Growth for Beginners* (World Scientific, Singapore, 1995).